

Effects of the surface structure and experimental parameters on the isopropanol decomposition catalyzed with sol–gel MgO

J.A. Wang^{a,1}, X. Bokhimi^a, O. Novaro^{a,*}, T. López^b, R. Gómez^b

^a *Institute of Physics, The National University of Mexico (UNAM) A.P. 20-364, 01000, Mexico D.F., Mexico*

^b *Department of Chemistry, Universidad Autónoma Metropolitana-I A.P. 55-534, 09340, Mexico D.F., Mexico*

Received 9 June 1998; accepted 22 December 1998

Abstract

Isopropanol decomposition was used as a probe reaction for characterizing the surface properties of sol–gel MgO catalysts. The specific surface area and the pore size distribution of the samples, calcined at different temperatures, were measured with the BET method. Acidity and basicity of the catalyst were determined by using TPD-NH₃ and TPD-CO₂ techniques. The total conversion and acetone selectivity depended on the experimental conditions. Increasing reaction temperature significantly improved the total conversion, but reduced acetone selectivity. The activity and acetone selectivity obtained at the initial reaction were higher than that obtained after 15 min and 30 min of reaction. When water was added in the reaction stream, hydroxyl groups were formed on the MgO surface, a remarkable enhancement of the conversion and of the acetone selectivity was observed. The structural defects and the specific surface area of the catalyst are also related to the activity and selectivity of the isopropanol decomposition. Two mechanisms were suggested for the explanation of acetone formation: in the case of water absent in the feed stream, the acetone was produced by the dehydrogenation route; in the case of water present in the reaction mixture, acetone was produced by the pathway of dehydrogenation accompanying the dehydration. © 1999 Elsevier Science B.V. All rights reserved.

Keywords: Isopropanol decomposition; Structural defects; MgO; Sol–gel catalyst; Acidic–basic properties; Dehydrogenation; Acetone

1. Introduction

A large number of papers have been published concerning the decomposition of alcohols

on oxide catalysts: ZnO [1–6], TiO₂ [7–20], and bimetallic oxides such as Al–Mg–O, Al–Ni–O, Ni–Si–O and V–Mo–O [21–23] and some multicomponent metal oxide MoO₃–Bi₂O₃–P₂O₅ [24]. Because the alcohol decomposition on solid catalysts occurs through two pathways: the dehydration which is generally catalyzed by the acidic sites and the dehydrogenation which is catalyzed by basic sites or both acidic and basic sites [25,26], this kind of decomposition has been used as an indicator of the surface acidic

* Corresponding author. Tel.: +52-5-622-5032; Fax: +52-5-616-1535; E-mail: novaro@fenix.ifisicacu.unam.mx

¹ Present address: Laboratorio de Catalísis y Materiales, SEPE-ESIQIE, Instituto Politécnico Nacional, UPALM, 07738 Mexico D.F., Mexico.

² Member of El Colegio Nacional, Mexico.

and basic sites of the solid catalysts. Therefore, when alcohol is decomposed on the catalysts, the relative reaction rates of dehydration and dehydrogenation can be used to characterize the acidic and basic properties of catalysts.

By studying a large series of single and bimetallic oxides in the isopropanol decomposition, Auroux and Gervasini [27,28] determined reaction-rate coefficients and the Arrhenius parameters for the dehydration and dehydrogenation of isopropanol. They found that the total number of acidic sites strongly affects the entropic activation parameters, but that the acidic strength mainly affects the activation energy. Therefore, by measuring and analyzing the reaction-rate coefficients and Arrhenius parameters, the surface acidic and basic properties can be diagnosed. The isopropanol decomposition was also successfully used to determine the TiO_2 or ZrO_2 segregation in $\text{TiO}_2\text{-SiO}_2$ [29] and $\text{ZrO}_2\text{-SiO}_2$ [30] oxides, respectively.

Although the above probe reactions have frequently been applied for the characterization of the surface acidic–basic sites for many years, there are still some open questions. For example, under some experimental conditions, the surface sites of the catalyst could be modified, altering the surface acidic or basic properties. In such case, the relationship between the basicity and acidity of the catalyst and the selectivity and the activity of the alcohol decomposition is difficult to be found. Rekoske and Barteau [12] and Lusvardi et al. [31] reported that during isopropanol decomposition on TiO_2 catalyst, acetone selectivity was remarkably improved by adding water or oxygen to the reactant stream. Other factors, particle size and phase concentration of the mixed oxide catalysts, should also be taken into account when the reaction selectivity must be correlated to the acidic and basic properties [32]. In a previous study [33], we found that when sol–gel alumina decomposes isopropanol, the basic sites determine the selectivity for the dehydrogenation to acetone; however, the selectivity for dehydration to propene is not strictly correlated to the acidic sites.

Solid catalysts have crystalline structures with vacancies, which are often related to the basic and acidic sites; therefore, in some cases, the structural defects are involved in the acid–basic catalytic reactions. These defects, however, are often neglected in catalytic studies, because of the difficulty to be characterized. It was found that isopropanol decomposition on sol–gel alumina catalysts is sensitive to the defects in its crystalline structure. For example, aluminum defects determine the selectivity for acetone dehydrogenation; but, oxygen defects, which are in connection to the coordinately unsaturated aluminum atoms in the catalyst, determine the bimolecular reaction to isopropylether [33].

In the present contribution, sol–gel MgO was the catalyst and isopropanol the alcohol. The effects of the experimental parameters such as the reaction temperature, reaction time and the composition of the reaction stream on the selectivity and activity of the isopropanol decomposition were studied. The temperature for the decomposition reaction ranged from 373 to 525 K, and the reaction time from 1 to 30 min. Water was added into the reaction mixture because it affects the selectivity and activity. Information of the structural defects was obtained by refining MgO crystalline structure via Rietveld technique [34].

2. Experimental

2.1. Catalyst preparation

Sol–gel MgO was synthesized by refluxing 5.72 g of $\text{Mg}(\text{OC}_2\text{H}_5)_2$ with 50 ml ethanol and 4.5 ml water. Synthesis reaction was catalyzed with 1 g $\text{H}_2\text{C}_2\text{O}_4$ at pH 5. The homogeneous mixture was refluxed at 353 K, stirring continuously, for 24 h until forming a gel. After vaporizing ethanol excess, the product was dried in air at 343 K to obtain a white powder. Before characterization, samples were calcined at 673, 873 and 1073 K.

Table 1
Data of specific surface area, pore volume and pore diameter of sol-gel MgO sample

| Calcination temperature (K) | Surface area (m ² /g) | Pore volume (cm ³ /g) | Pore diameter (Å) |
|-----------------------------|----------------------------------|----------------------------------|-------------------|
| 673 | 199 | 0.7450 | 150 |
| 873 | 267 | 1.1279 | 143 |
| 1073 | 163 | 0.3457 | 320 |

2.2. Measurements of surface area, pore volume and pore size distribution

Specific surface areas and pore size distribution were measured with an ASAP 2000 analyzer, from the isotherm adsorption of liquid nitrogen. Before the measurement, the samples were treated at 673 K for 1 h.

2.3. Acidity and basicity analysis

Acidic and basic sites were measured by temperature-programmed desorption of ammonia and carbon dioxide (TPD-NH₃ and TPD-CO₂). To desorb impurities, before adsorption, the samples were heated at 773 K, in a He stream, for 30 min. After that, they were saturated with ammonia or carbon dioxide for 30 min at 283 K. Extra adsorbed species were eliminated by flowing dry He at the same temperature. Desorption signal was recorded with a thermal-conducting detector while samples were heated.

2.4. Catalytic activity test

Catalytic activity test was performed in a flowing microreactor linked with a gas-chromatograph (MR-GC). Isopropanol (99.9%, H₂O% ≤ 0.06, Aldrich) was contained in a double H-type saturator imbedded in a recipient with a mixture of ice and water. In all tests, nitrogen was used as carrier. The partial pressure of 2-propanol was controlled by varying the temperature of the ice–water mixture. Typically, 50 mg catalyst samples were used in the activity measurements. Total conversion of isopropanol was acquired by measuring the con-

centrations of isopropanol before and after the reaction. To avoid the complex effects of the water produced by the reaction, the total conversion was controlled to less than 15%. This was done by maintaining the reaction temperature below 523 K. In Section 4, we will discuss in more detail the effects of added water; but, overlook the water produced by the reaction.

3. Results

3.1. Specific surface area, pore volume and pore size distribution

Specific surface area, pore volume and pore size distribution are shown in Table 1. When the samples were calcined at different temperatures, their surface properties changed. The surface specific area increased from 199 m²/g at 673 K to 267 m²/g at 873 K, but decreased to 163 m²/g at 1073 K. The pore volume increased from 0.7450 cm³/g at 673 K to 1.1279 cm³/g at 873 K, and then decreased to 0.3457 cm³/g at 1073 K. These results show that the surface properties of the samples are strongly affected by the thermal process.

3.2. Acidity and basicity of the samples

Acid and basic properties of the MgO samples were characterized with NH₃-TPD and CO₂-TPD (Table 2). Only the sample calcined at 673 K adsorbed ammonia (134 μmol/g). This can be explained by assuming that the sample calcined at 673 K had acidic sites, but they were absent in the samples calcined at 873 and 1073 K due to the changes of the surface properties.

Table 2
Data of TPD-NH₃ and TPD-CO₂

| Temperature (K) | Amount of adsorbed NH ₃ (μmol/g) | Amount of adsorbed CO ₂ (μmol/g) |
|-----------------|---|---|
| 673 | 134 | 1398 |
| 873 | 0 | 1182 |
| 1073 | 0 | 914 |

Table 3

Total conversion of isopropanol decomposition at different reaction temperatures on MgO calcined at 673 K

| Reaction temperature (K) | Total conversion (%) | | | | | |
|--------------------------|----------------------|--------|--------|------------|--------|--------|
| | Without water | | | With water | | |
| | 1 min | 15 min | 30 min | 1 min | 15 min | 30 min |
| 373 | 0.08 | 0.04 | 0.04 | 0.13 | 0.07 | 0.08 |
| 423 | 0.17 | 0.05 | 0.06 | 0.25 | 0.20 | 0.19 |
| 448 | 0.32 | 0.29 | 0.30 | 0.47 | 0.44 | 0.45 |
| 473 | 1.54 | 1.39 | 1.33 | 1.79 | 1.68 | 1.66 |
| 498 | 2.71 | 2.58 | 2.56 | 3.02 | 2.93 | 2.79 |
| 523 | 13.90 | 10.54 | 11.02 | 14.48 | 13.01 | 13.12 |

Samples had high capacity for adsorbing CO₂ molecules, showing the basic character of sol-gel MgO. When calcining temperature was increased from 673 K to 873 and to 1073 K, the amount of adsorbed CO₂ decreased from 1398 μmol/g to 1182 and 914 μmol/g, which corresponds to a diminishing of the number of the basic sites.

3.3. Activity and selectivity of isopropanol decomposition

For measuring the activity for isopropanol decomposition, we studied its conversion as a function of reaction time, reaction temperature, and water in the fed stream. Tables 3–5 show the total conversions on samples calcined at 673, 873 and 1073 K.

At a constant reaction temperature, after 1 min reaction time, the total conversion was

Table 4

Total conversion of isopropanol decomposition at different reaction temperatures on MgO calcined at 873 K

| Reaction temperature (K) | Total conversion (%) | | | | | |
|--------------------------|----------------------|--------|--------|------------|--------|--------|
| | Without water | | | With water | | |
| | 1 min | 15 min | 30 min | 1 min | 15 min | 30 min |
| 373 | 0.06 | 0.05 | 0.05 | 0.08 | 0.06 | 0.06 |
| 423 | 0.13 | 0.09 | 0.08 | 0.21 | 0.17 | 0.16 |
| 448 | 0.37 | 0.32 | 0.30 | 0.44 | 0.36 | 0.38 |
| 473 | 0.98 | 0.75 | 0.77 | 1.53 | 1.44 | 1.39 |
| 498 | 1.81 | 1.73 | 1.66 | 2.04 | 1.89 | 1.81 |
| 523 | 5.08 | 4.31 | 4.47 | 6.75 | 5.50 | 5.62 |

Table 5

Total conversion of isopropanol decomposition at different reaction temperatures on MgO calcined at 1073 K

| Reaction temperature (K) | Total conversion (%) | | | | | |
|--------------------------|----------------------|--------|--------|------------|--------|--------|
| | Without water | | | With water | | |
| | 1 min | 15 min | 30 min | 1 min | 15 min | 30 min |
| 373 | 0.04 | 0.02 | 0.02 | 0.08 | 0.06 | 0.05 |
| 423 | 0.08 | 0.05 | 0.06 | 0.29 | 0.21 | 0.19 |
| 448 | 0.20 | 0.16 | 0.15 | 0.33 | 0.28 | 0.29 |
| 473 | 0.44 | 0.34 | 0.30 | 0.74 | 0.53 | 0.55 |
| 498 | 1.11 | 0.79 | 0.77 | 1.86 | 1.47 | 1.52 |
| 523 | 4.38 | 4.19 | 4.03 | 5.68 | 5.03 | 5.12 |

higher than after 15 and 30 min. No significant difference was observed in the conversions obtained after 15 min and 30 min. When the reaction temperature was increased, the total conversion of isopropanol decomposition also increased.

When water was introduced into the reaction stream, the isopropanol decomposition reaction was significantly affected, for example, the total conversions was increased compared to that obtained in the case of water absent in the fed stream (Tables 3–5).

The effects of the experimental parameters on the selectivity of acetone were also analyzed, obtaining the following information (Figs. 1–4): 1. When the reaction temperature was increased, acetone selectivity decreased (Figs. 1 and 2).

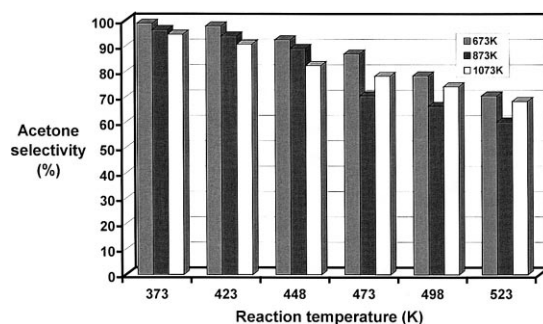


Fig. 1. The acetone selectivity as function of the reaction temperature. The reaction was carried out in the case of water stream present in the fed mixture. The data were obtained after 15 min of reaction.

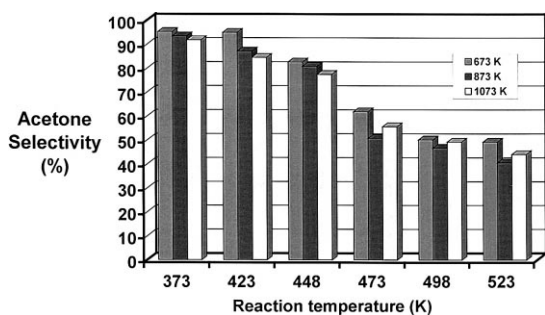


Fig. 2. The acetone selectivity as function of the reaction temperature. The reaction was carried out in the case of water stream absent in the fed mixture. The data were obtained after 15 min of reaction.

2. The acetone selectivity, obtained after 1 min of reaction, was higher than the one obtained after 15 and 30 min of reaction (Fig. 3).
3. The water introduced into the reactant mixture remarkably improved acetone selectivity (Fig. 4).

4. Discussion

4.1. Basic site, structural defect and acetone selectivity

From the refinement of MgO crystalline structure with the Rietveld technique, it was observed that the lattice had magnesium defects [34]. On the one hand, the cationic defects are often related to the basic sites in the sample due

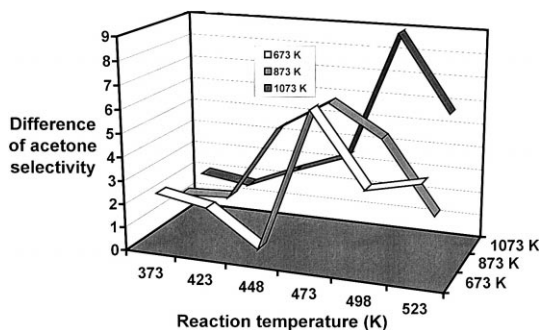


Fig. 3. Difference of the acetone selectivity between 1 min and 15 min of reaction as function of the reaction temperature. The reaction was carried out in the case of water stream absent in the fed reaction mixture.

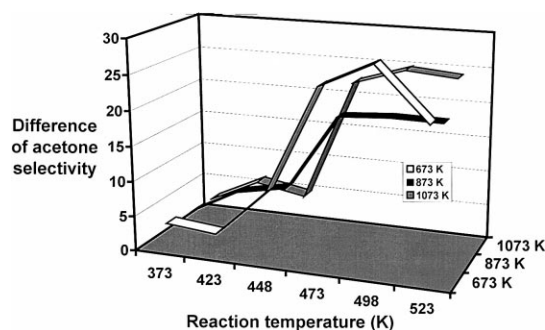


Fig. 4. Difference of the acetone selectivity between water stream presence and absence in the fed reaction mixture. The data were obtained after the reaction was carried out for 15 min.

to its electron-rich character. On the other hand, the decomposition of isopropanol, in particular, the selectivity of the dehydrogenation to acetone, is also related to the basic and/or acidic properties. Therefore, the study of the relationship between the basic sites, structural defects and the activity or selectivity of isopropanol decomposition is very interesting. Table 6 shows the data of magnesium basic sites, defect sites and acetone selectivity.

When the calcining temperature was increased from 673 K to 873 and 1073 K, the concentration of magnesium defect per unit lattice cell decreased from 8.17% to 7.21 and 6.90%. Similarly, the amount of adsorbed CO_2 also decreased from 1398 $\mu\text{mol/g}$ at 673 K to 1182 $\mu\text{mol/g}$ at 873 K and 914 $\mu\text{mol/g}$ at 1073 K. This result shows that the cationic defects are related to the basicity and some of the basic sites are yielded from the cationic defects in MgO catalyst.

From the data shown in Tables 3–5, it is found that not only the calcining temperature of the sample affects the acetone selectivity, but also the reaction temperatures. At low reaction temperatures (< 473 K), the acetone selectivity sequence is $S_{673} > S_{873} > S_{1073}$ (S denotes the acetone and the numbers correspond to the annealing temperatures), which is the same sequence as basic sites and cationic defects as functions of calcining temperature of the samples. This result shows that the acetone selectivity

Table 6

Data of magnesium vacancies, basic sites and acetone selectivity for different MgO samples

| Calcining temperature (K) | Magnesium defects (%) | Basic sites (N/nm ²) | Acetone selectivity (%) ^a | | | |
|---------------------------|-----------------------|----------------------------------|--------------------------------------|-------|-------|--------------------|
| | | | 373 K | 423 K | 473 K | 523 K ^b |
| 673 | 8.17 | 0.70 | 95.3 | 95.0 | 61.2 | 49.3 |
| 873 | 7.21 | 0.44 | 93.5 | 87.2 | 50.0 | 40.6 |
| 1073 | 6.90 | 0.56 | 91.9 | 84.6 | 55.4 | 44.1 |

^aThe acetone selectivity was measured after 15 min of reaction. The reaction mixture is without water.^bThe reaction temperature.

ity depends on the basicity and probably relates to the cationic defects of the catalyst.

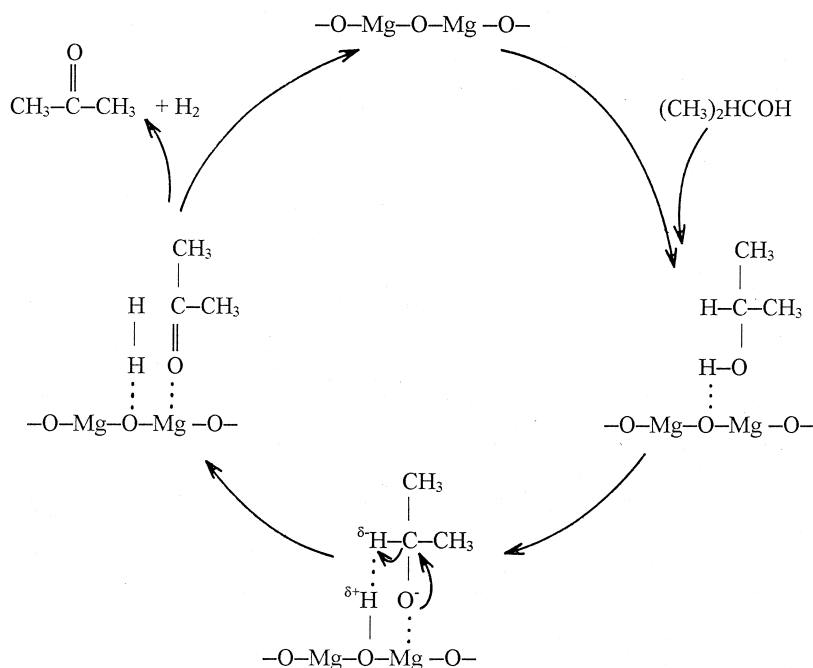
When the specific surface area of the sample was taken into account, the number of the total basic sites per unit surface area was found to decrease from 0.7/nm² in the sample calcined at 673 K to 0.44/nm² at 873 K and then increase to 0.56/nm² at 1073 K. The sample calcined at 873 K has the largest surface area but with the lowest basic number per nm². It is noted that the acetone selectivity on the sample calcined at 873 K is the lowest in the three samples, differing from the traditional idea that the large specific surface area is favorable for the reaction. It indicates that the large specific surface dilutes the basic site concentration. The dilution effect gives rise to a decrease in acetone selectivity. At high reaction temperatures (> 473 K), the order of both the acetone selectivity and the number of the basic sites per unit surface area showing on different samples is $S_{673} > S_{1073} > S_{873}$, the dilution effect, therefore, remarkably affects the acetone formation.

To explain the acetone formation, Szabó and Jóvmacht [35] once presented a likely mechanism, in which they suggested the α -H is dissociated to H⁻ and it links to an adjacent cation. The H⁻ reacts with another H⁺, which is bonded on a lattice oxygen ion, to form molecular hydrogen. The question is that in the suggested mechanism the lattice oxygen ion and cationic ion are not neighbors, separating by one cationic ion and a lattice oxygen ion. The distance between them seems too long, which does not favor for hydrogen formation.

As discussed above, because the lattice oxygen ions in metallic oxide are electron-donors and hence show the basic character, they must be the active sites for acetone formation during isopropanol decomposition process. Therefore, we assumed that lattice oxygen sites serve as reaction centers. Due to the interaction between the lattice oxygen ion and the hydrogen ion in H–O bond of the isopropanol molecule, the H–O bond is broken, producing a hydrogen ion (H⁺) and alkoxide carbanion species ((CH₃)₂HCO⁻). The produced hydrogen ion (H⁺) is trapped by an oxygen lattice ion. Simultaneously the alkoxide carbanion species interacts with the adjacent magnesium ion. Afterwards, by breaking the α -hydrogen–carbon bond, the α -hydrogen reacts with the hydrogen ion trapped in the oxygen lattice ion, forming molecular hydrogen. The adsorbed acetone molecule is yielded. The adsorbed acetone and hydrogen molecules desorb from the surface of the catalyst, regenerating the active site. This suggested mechanism is presented in Scheme 1.

4.2. The effects of the reaction time

To study the effect of the reaction time on the selectivity and activity of isopropanol decomposition, at different reaction temperatures, we first detected the conversion and the selectivity at initial time (after 1 min of reaction). Afterwards, the conversion and selectivity were determined after 15 min and 30 min of reaction. All the data are shown in Tables 3–5 and Figs. 1–4.



Scheme 1. Lattice oxygen serves for acetone formation. Acetone is generated from the dehydrogenation pathway.

After 1 min of reaction, the total conversion was found to be higher than the one observed after 15 min and 30 min (Tables 3–5). The studies of the deactivation kinetics show that the isopropanol decomposition is a reaction accompanied with carbonaceous materials deposition on the reaction centers [30]. Therefore, the decrease of the total conversion with the reaction time can be understood by the deactivation of the catalyst by the coke deposition on the active sites after some time of reaction.

At an initial time of reaction and a fixed reaction temperature, the selectivity of dehydrogenation to acetone is higher compared with the results obtained after 15 or 30 min (Fig. 3). With respect to the concept of basicity, the cationic defects are connected to the strong basic sites due to its electron-rich character. In the fresh surface, some isopropanol molecules can be selectively adsorbed on the defect tracks and decomposed to form acetone. During the reaction, the stronger basic centers are readily covered with produced coke. The deposited coke would have complex effect on acetone selectiv-

ity. On the one hand, it can improve acetone selectivity by tracking hydrogen ions; on the other hand, it may poison the active sites for acetone formation, resulting in a reduction of acetone selectivity. In our case, because a slight decrease in acetone selectivity with the reaction time at variously fixed temperature was observed (Fig. 3), the poisoning function of coke seems to be more significant than its enhancing function.

4.3. The effects of the adsorbed water

When water was introduced into the reactant stream, the selectivity of dehydrogenation to acetone was markedly improved (Fig. 4). These results disagree with the common sense that the water molecules that added in the inlet stream would occupy some reaction active sites, inhibiting the adsorption of isopropanol on these sites and decreasing the total conversion. The adsorbed water on the catalyst's surface may produce bounded water and surface hydroxyl ions when it is thermally treated [12,31]. There-

fore, a significant difference between the reactant mixtures with and without water is the presence of hydroxyl ions on the surface when water is added.

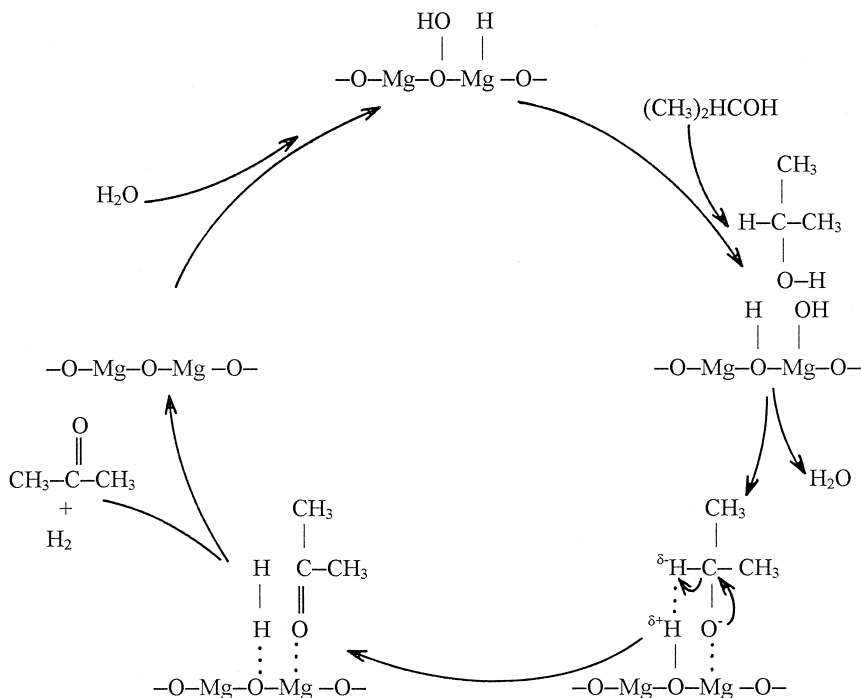
When isopropanol decomposition occurs on this kind of surface, the hydroxyl ions are directly involved in the reaction of forming acetone. Therefore, adding water in the fed stream produces additional active sites for the acetone generation. Based on this idea, Scheme 2 is also a plausible route for producing acetone when water is present in the fed stream.

In Scheme 2, the hydroxyl groups and hydrogen ions bonded on the lattice oxygen are suggested to exist on the MgO surface, which are involved in the acetone formation. First, the hydrogen ion from the OH group in isopropanol molecule reacts with the hydroxyl ion linked to the cation in MgO surface, producing molecular water and an alkoxide carbanion species. Then, the alkoxide carbanion species interacts with an adjacent cation. In such case, the active α -H in the alkoxide carbanion species reacts with the hydrogen ion linked with an oxygen lattice ion

to yield the molecular hydrogen. After giving the α -H ion, alkoxide carbanion transfers to the acetone molecule.

The formation of acetone from Scheme 1 differs from that produced in Scheme 2. In Scheme 1, acetone is yielded from the dehydrogenation routes. However, in Scheme 2, acetone is yielded from the dehydrogenation pathway accompanied by the dehydration. Therefore, adding water in the fed stream mainly produces additional hydroxyl groups linked on the catalyst surface. These bonded hydroxyl ions promote the generation of acetone by the dehydration and dehydrogenation routes.

At reaction temperatures below 423 K, since the differences of acetone selectivity between the inlet stream with and without water was less than 4%, the water effect on the acetone selectivity was not significant (Fig. 4). When the reaction temperature was increased, the differences of the acetone selectivity became big; above 473 K, this difference significantly increased. However, at 523 K, the difference slightly decreased. These results show that the



Scheme 2. Acetone is generated from the dehydrogenation route accompanying the dehydration when water is present in the fed stream.

water influences on the acetone selectivity are sensitive to the reaction temperature.

It is noteworthy that when the reaction temperature reached 523 K, the total conversions are higher than 5% for the samples calcined at 873 and 1073 K and more than 10% for the sample calcined at 673 K. In the case of high conversion, reaction produced relatively large amounts of water in situ, which cannot be overlooked. The slight drop in the difference of acetone selectivity at 523 K indicates that the influence of water seem also to be related to the adsorption and desorption of water, which is strongly affected by the temperature. The complex influences of water produced in situ during the isopropanol decomposition will be reported in a future paper.

5. Conclusions

Isopropanol decomposition on sol–gel MgO was strongly affected by the variations of the experimental parameters: reaction temperature, adsorption or reaction time and fed mixtures. Increasing the reaction temperature improved the total conversion, but reduced the acetone selectivity. At the beginning of the reaction, both the acetone selectivity and the total conversion were higher than after 15 and 30 min.

When water was added to the fed stream, the selectivity to acetone was significantly promoted, mainly by improving the dehydrogenation route accompanying the dehydration due to the formation of hydroxyl groups on the catalyst surface.

The structural defects, due to its electron-rich character, were found to be connected with the basic sites, which probably served for isopropanol decomposition reaction, especially, for forming acetone. The large specific surface area of the catalyst calcined at 873 K gives rise to a dilution to the basic site concentration, decreasing the acetone selectivity when the reaction temperature was higher than 473 K.

Acknowledgements

J.A. Wang, would like to thank the financial support from the CONACyT, Mexico, for his postdoctoral study at the Institute of Physics, of The National University of Mexico (UNAM).

References

- [1] O.V. Krylov, *Catalysis by Nonmetals*, Academic Press, New York, 1970, 115.
- [2] O. Koga, T. Onishi, K.C. Waugh, *JCS Faraday 1* (76) (1980) 19.
- [3] M. Bowker, R.W. Petts, K.C. Waugh, *JCS Faraday Trans. 1* (81) (1985) 3070.
- [4] M. Bowker, H. Houghton, K.C. Waugh, *JCS Faraday Trans. 1* (78) (1982) 2573.
- [5] M. Bowker, H. Houghton, K.C. Waugh, T. Giddings, M. Green, *J. Catal.* 84 (1983) 252.
- [6] K.C. Waugh, M. Bowker, R.W. Petts, H.D. Vandervell, J. O'Malley, *Appl. Catal.* 25 (1986) 121.
- [7] S.A. Larson, J.A. Widegren, J.L. Falconer, *J. Catal.* 157 (1995) 611.
- [8] R.I. Bickley, G. Munuera, F.S. Stone, *J. Catal.* 31 (1973) 398.
- [9] R.I. Bickley, R.K.M. Jayanty, *Discuss. Faraday Soc.* 58 (1974) 194.
- [10] V.S. Lusvardi, M.A. Barteau, W.R. Dolinger, W.E. Farneth, *J. Phys. Chem.* 100 (1996) 18183.
- [11] V.S. Lusvardi, M.A. Barteau, W.E. Farneth, *J. Catal.* 153 (1995) 41.
- [12] J.E. Rekoske, M.A. Barteau, *J. Catal.* 165 (1997) 57.
- [13] A. Gervasini, A. Auroux, *J. Catal.* 131 (1991) 190.
- [14] J. Cunningham, B.K. Hodnett, M. Ilyas, J. Tobin, E.L. Leahy, J.L.G. Fierro, *Faraday Discussions* 72 (1981) 283.
- [15] A.I. Biaglow, R.J. Gorte, S. Srinivasan, A.K. Datye, *Catal. Lett.* 13 (1992) 313.
- [16] K.S. Kim, M.A. Barteau, *Surf. Sci.* 223 (1989) 13.
- [17] K.S. Kim, M.A. Barteau, *J. Mol. Catal.* 63 (1990) 103.
- [18] E.A. Taylor, G.L. Griffin, *J. Phys. Chem.* 92 (1988) 477.
- [19] Y. Suda, T. Morimoto, M. Nagao, *Langmuir* 3 (1987) 99.
- [20] K.S. Kim, M.A. Barteau, *Langmuir* 6 (1988) 945.
- [21] A. Gervasini, J. Fenyvesi, A. Auroux, *Catal. Lett.* 43 (1997) 219.
- [22] A. Gervasini, G. Bellussi, J. Fenyvesi, A. Auroux, *J. Phys. Chem.* 99 (1995) 5117.
- [23] M. Ai, S. Suzuki, *Nippon Kagaku Kaishi*, (1973) 260.
- [24] M. Mamour, T. Ikawa, *J. Catal.* 40 (1975) 203.
- [25] M. Ai, S. Suzuki, *Bull. Jpn. Petrol. Inst.* 16 (1974) 118.
- [26] M. Ai, S. Suzuki, *Shokubai* 15 (1973) 159.
- [27] A. Auroux, A. Gervasini, *J. Phys. Chem.* 94 (1990) 6317.
- [28] A. Gervasini, A. Auroux, *J. Catal.* 131 (1991) 190.
- [29] A.I. Biaglow, R.J. Gorte, S. Srinivasan, A.K. Datye, *Catal. Lett.* 13 (1992) 313.

- [30] R. Gomez, T. López, F. Tzompantzi, E. Garciafigueroa, D.W. Acosta, O. Novaro, *Langmuir* 13 (1997) 970.
- [31] V.S. Lusvardi, M.A. Barteau, W.R. Dolinger, W.E. Farneth, *J. Phys. Chem.* 100 (1996) 18183.
- [32] R. Portillo, T. López, R. Gómez, Bokhimi, A. Morales, O. Novaro, *Langmuir* 12 (1996) 40.
- [33] J.A. Wang, X. Bokhimi, O. Novaro, T. López, F. Tzompantzi, R. Gómez, J. Navarrete, M.E. Llanos, E. López-Salinos, *J. Mol. Catal.* (in press).
- [34] J.A. Wang, O. Novaro, X. Bokhimi, T. López, R. Gómez, J. Navarrete, M.E. Llanos, E. López-Salinas, *J. Phys. Chem.* 38 (1997) 7448.
- [35] Z. Szabó, B. Jóvmacht, *J. Catal.* 39 (1975) 225.